IMMUNOLOGY   ORIGINAL ARTICLE

Alteration of *N*-glycosylation in the kidney in a mouse model of systemic lupus erythematosus: relative quantification of *N*-glycans using an isotope-tagging method

Noritaka Hashii,[1,2] Nana Kawasaki,[1,2] Satsuki Itoh,[1] Yukari Nakajima,[1,2] Toru Kawanishi[1] and Teruhide Yamaguchi[1]

[1]*Division of Biological Chemistry and Biologicals, National Institute of Health Sciences, Setagaya-ku, Tokyo, Japan, and* [2]*Core Research for Evolutional Science and Technology (CREST) of the Japan Science and Technology Agency (JST), Kawaguchi City, Saitama, Japan*

Summary

Changes in the glycan structures of some glycoproteins have been observed in autoimmune diseases such as systemic lupus erythematosus (SLE) and rheumatoid arthritis. A deficiency of α-mannosidase II, which is associated with branching in *N*-glycans, has been found to induce SLE-like glomerular nephritis in a mouse model. These findings suggest that the alteration of the glycosylation has some link with the development of SLE. An analysis of glycan alteration in the disordered tissues in SLE may lead to the development of improved diagnostic methods and may help to clarify the carbohydrate-related pathogenic mechanism of inflammation in SLE. In this study, a comprehensive and differential analysis of *N*-glycans in kidneys from SLE-model mice and control mice was performed by using the quantitative glycan profiling method that we have developed previously. In this method, a mixture of deuterium-labelled *N*-glycans from the kidneys of SLE-model mice and non-labelled *N*-glycans from kidneys of control mice was analysed by liquid chromatography/mass spectrometry. It was revealed that the low-molecular-mass glycans with simple structures, including agalactobiantennary and paucimannose-type oligosaccharides, markedly increased in the SLE-model mouse. On the other hand, fucosylated and galactosylated complex type glycans with high branching were decreased in the SLE-model mouse. These results suggest that the changes occurring in the *N*-glycan synthesis pathway may cause the aberrant glycosylations on not only specific glycoproteins but also on most of the glycoproteins in the SLE-model mouse. The changes in glycosylation might be involved in autoimmune pathogenesis in the model mouse kidney.

Keywords: isotope-tagging method; liquid chromatography/multiple-stage mass spectrometry; systemic lupus erythematosus

Introduction

Glycosylation is one of the most common post-translational modifications[1,2] and contributes to many biological processes, including protein folding, secretion, embryonic development and cell–cell interactions.[3] Alteration of glycosylation is associated with several diseases, including inflammatory responses and malignancies;[4–6] for instance, significant increases in fucosylation and branching are found in ovarian cancer and lung cancer.[7] Additionally, the carbohydrate structure changes from type I glycans (Galβ1-3GlaNAc) to type II glycans (Galβ1-4GalNAc) in

carcinoembryonic antigen in colon cancer.[8] Furthermore, an increase in biantennary oligosaccharides lacking galactose (Gal) was found on immunoglobulin G (IgG) in systemic lupus erythematosus (SLE) and rheumatoid arthritis,[9–11] and agalactoglycans are used for the early diagnosis of rheumatoid arthritis.[12]

Systemic lupus erythematosus is an autoimmune disease characterized as chronic and as a systemic disease, with symptoms such as kidney failure, arthritis and erythema. In addition to the known changes in glycosylation on IgG, there have been several reports on the association between glycosylation and inflammation in SLE and rheumatoid

arthritis.[13–15] A deficiency of α-mannosidase II (αM-II), which is associated with branching in *N*-glycans, has been found to induce human SLE-like glomerular nephritis in a mouse model.[16] Green *et al.* reported that branching structures of *N*-glycan in mammals are involved in protection against immune responses in autoimmune disease pathogenesis.[17] Although there is no direct evidence that alteration of glycosylation is the upstream event in the pathogenesis of SLE, these findings suggest that changes in the glycan structure may be involved in the inflammatory-related autoimmune disorder. Glycosylation analysis may lead to the development of improved diagnostic methods and may help to clarify the carbohydrate-related pathogenic mechanism of inflammation in SLE.

Mass spectrometry (MS) and liquid chromatography/ mass spectrometry (LC/MS) are the most prevalent strategies for identifying disease-related glycans in glycomics.[18–20] Aberrant glycosylations in some disease samples have been found by comparing mass spectra or chromatograms between normal and disease samples; however, because of the tremendous heterogeneities of the sugar moiety in glycoprotein as well as the low reproducibility of LC/MS, accurate quantitative analysis is difficult using MS and LC/MS alone. To overcome these problems, we previously developed the stable isotope-tagging method for the quantitative profiling of glycans using 2-amino-pyridine (AP).[21] After the glycans are released from sample and the reference glycoproteins are derivatized to pyridyl amino (d_0-PA) glycans and to tetra-deuterium-labelled pyridyl amino (d_4-PA) glycans, respectively, a mixture of both d_0-PA and d_4-PA glycans was subjected to LC/MS, and the levels of individual glycans were calculated from the intensity ratios of d_0-glycan and d_4-glycan molecular ions (Fig. 1a). Recently, alternative isotope-tagging methods using deuterium-labelled compounds, such as 2-aminobenzoic acid its derivatives, and permethylation, have been proposed by other groups.[22–24] All of these studies prove the utility of isotope-tagging methods for the quantitative analysis of glycosylation.

In the present study, we used the isotope-tagging method to analyse changes in *N*-glycosylation in the disordered kidney in an SLE mouse model. We used an MRL/MpJ-lpr/lpr (MRL-lpr) mouse which lacks the Fas antigen gene.[25–27] The MRL-lpr mouse is known to naturally develop SLE-like glomerular nephritis and is widely used in SLE studies. MRL/MpJ-+/+ (MRL-+/+) mice were used as controls.

Materials and methods

Materials

The kidneys of the SLE-model mice (MRL-lpr) and control mice (MRL-+/+) (*n* = 3) were purchased from Japan SLC, Inc. (Hamamatsu, Japan). Thermolysin (EC 3.4.24.27), originating from *Bacillus thermoproteolyticus*
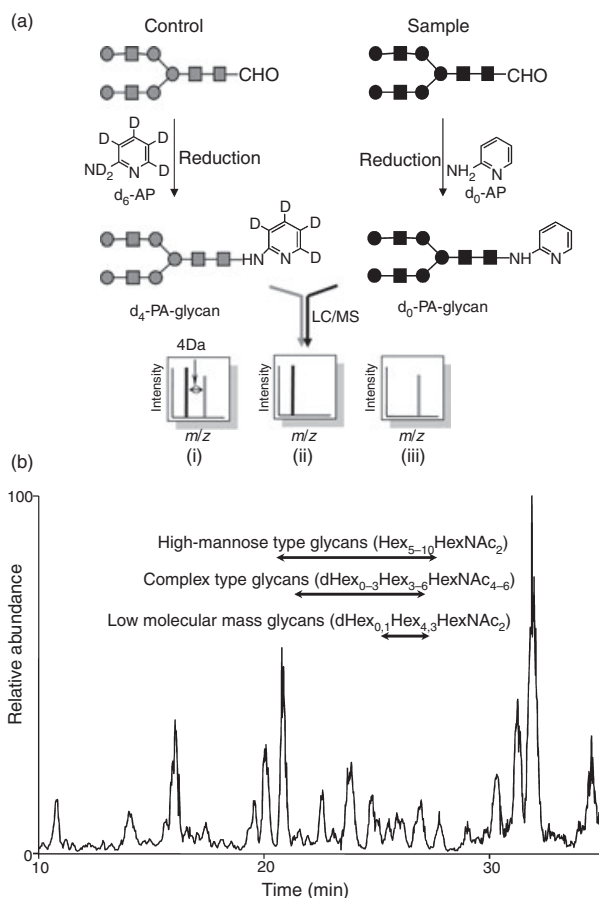

Figure 1. (a) Quantitative glycan profiling using the stable isotope-tagging method and liquid chromatography/mass spectrometry (LC/MS). (i) sample = control, (ii) sample > control, (iii) sample < control. (b) Total ion chromatogram obtained by a single scan (*m/z* 700–2000) of the d_0-glycan and d_4-glycan mixture.

Rokko, was purchased from Daiwa Kasei (Shiga, Japan). Glycopeptidase A (PNGase A) was obtained from Seikagaku Kogyo Corporation (Tokyo, Japan). Non-deuterium-labelled 2-aminopyridine (d_0-AP) and deuterium-labelled 2-aminopyridine (d_6-AP) were purchased from Takara Bio (Otsu, Japan) and Cambridge Isotope Laboratories (Andover, MA), respectively.

Sample preparation

Mouse kidneys were filtered using a cell strainer (70 μm; BD Biosciences, San Jose, CA) and contaminating blood cells in the kidney cells were burst in 140 mM NH_4Cl–Tris buffer (pH 7·2). The surviving kidney cells were washed three times with phosphate-buffered saline containing a mixture of protease inhibitors (Wako, Tokyo, Japan) and dissolved in guanidine–HCl buffer (8 M guanidine–HCl, 0·5 M Tris–HCl, pH 8·6) containing a mixture of protease inhibitors by vortexing at 4°. The protein concentration was measured using a 2-D Quant Kit (GE Healthcare

Bio-Sciences, Uppsala, Sweden). The protein solution (200 μg proteins) was incubated with 40 mM dithiothreitol at 65° for 30 min. Freshly prepared sodium iodoacetate (final concentration, 96 mM) was added to the sample solution, and the mixture was incubated at room temperature for 40 min in the dark. The reaction was stopped by adding cystine (6 mg/ml in 2 M HCl) in an amount equal to the amount of dithiothreitol. The solution containing carboxymethylated proteins was diluted in four times its volume of H_2O, and the mixture was incubated with 0·1 μg of thermolysin at 65° for 1 hr. After terminating the reaction by boiling, the reaction mixture was diluted in four times its volume of 0·2 M acetate buffer. The *N*-linked glycans were released by treatment with PNGase A (1 mU) at 37° for 16 hr and were desalted using an EnviCarb C cartridge (Supelco, Bellefonte, PA).

Labelling of N-glycans with d_0-AP and d_6-AP

Glycans released from the SLE-model mouse cells were incubated in acetic acid (20 μl) with 12·5 M d_0-AP at 90° for 1 hr. Next, 3·3 M borane–dimethylamine complex reducing reagent in acetic acid (20 μl) was added to the solution and the mixture was incubated at 80° for 1 hr. Excess reagent was removed by evaporation, and d_0-PA glycans were desalted using an EnviCarb C cartridge, concentrated in a SpeedVac and reconstituted in 20 μl of 5 mM ammonium acetate (pH 9·6). Glycans released from the control mouse were labelled with d_6-AP in a similar manner. The resulting d_4-PA glycans were combined with d_0-PA glycans, which were prepared from an equal amount of proteins.

On-line liquid chromatography/mass spectrometry

The sample solution (4 μl) was injected into the LC/MS system through a 5-μl capillary loop. The d_0-PA and d_4-PA glycans were separated in a graphitized carbon column (Hypercarb, 150 × 0·2 mm, 5 μm; Thermo Fisher Scientific, Waltham, MA) at a flow rate of 2 μl/min in a Magic 2002 LC system (Michrom Bioresources, Auburn, CA). The mobile phases were 5 mM ammonium acetate containing 2% acetonitrile (pH 9·6, A buffer) and 5 mM ammonium acetate containing 90% acetonitrile (pH 9·6, B buffer). The PA-glycans were eluted with a linear gradient of 5–45% of B buffer for 90 min.

Mass spectrometric analysis of PA glycans was performed using a Fourier transform ion cyclotron resonance/ion trap mass spectrometer (FT-ICR-MS, LTQ-FT; Thermo Fisher Scientific) equipped with a nanoelectrospray ion source (AMR, Tokyo, Japan). For MS, the electrospray voltage was 2·0 kV in the positive ion mode, the capillary temperature was 200°, the collision energy was 25% for MS^n experiment, and the maximum injection times for FT-ICR-MS and MS^n were 1250 and 50 milliseconds, respectively. The resolution of FT-ICR-MS was 50 000, the scan time (*m/z* 700–2000) was approximately 0·2 seconds, dynamic exclusion was 18 seconds, and the isolation width was 3·0 U (range of precursor ions ± 1·5).

Results

Quantitative profiling of kidney oligosaccharides in the SLE-model mouse

The recovery of oligosaccharides from whole tissues and cells is generally low because of the insolubility of the membrane fraction and possible degradation of the glycans. To improve the recovery of *N*-glycans from kidney cells, whole cells were dissolved in guanidine hydrochloride solution, and all proteins, including membrane proteins, were digested into peptides and glycopeptides with thermolysin. The *N*-glycans were then released from the glycopeptides with PNGase A, which is capable of liberating *N*-linked oligosaccharides even at the N- and/or C-terminals of peptides. The *N*-linked oligosaccharides from the SLE-model mice and control mice were labelled with d_0-AP and d_6-AP, respectively. The mixture of labelled glycans derived from an equal amount of proteins was subjected to quantitative glycan profiling using LC/MS^n.

Figure 1(b) shows the total ion chromatogram obtained by a single mass scan (*m/z* 700–2000) of the glycan mixture in the positive ion mode. Although the MS data contain many MS spectra derived from contaminating low-molecular-weight peptides, the MS/MS spectra of oligosaccharides could be sorted based on the existence of carbohydrate-distinctive ions, such as $HexHexNAc^+$ (*m/z* 366) and $Hex(dHex)HexNAc^+$ (*m/z* 512). The monosaccharide compositions of the precursor ions were calculated from accurate *m/z* values acquired by FT-ICR-MS. Oligosaccharides found at 25–27 min were assigned to low-molecular-mass glycans consisting of $dHex_{0,1}Hex_{4,3}HexNAc_2$ (dHex, deoxyhexose; Hex, hexose; HexNAc, *N*-acetylhexosamine). High-mannose-type glycans, which consist of $Hex_{5-10}HexNAc_2$, were located at 20–28 min; complex-type glycans ($dHex_{0-3}Hex_{3-6}HexNAc_{4-6}$) were found at 21–27 min. Figure 2(a) shows the relative intensities of the molecular ions of *N*-glycans in the SLE-model mouse, which may correspond roughly to the levels of individual *N*-glycans. More than half of all glycans were complex-type oligosaccharides, and the most prominent glycan was $dHex_3Hex_5HexNAc_5$. Man-9 ($Hex_9HexNAc_2$) was the second most common oligosaccharide. Nearly one-quarter of the glycans were low-molecular-mass glycans, and $dHex_1Hex_2HexNAc_2$ was the third most abundant glycan in the SLE-model mouse. The rate of percentage change in individual glycans between the SLE-model mice and control mice was calculated from the intensity ratio of d_0-glycan and d_4-glycan
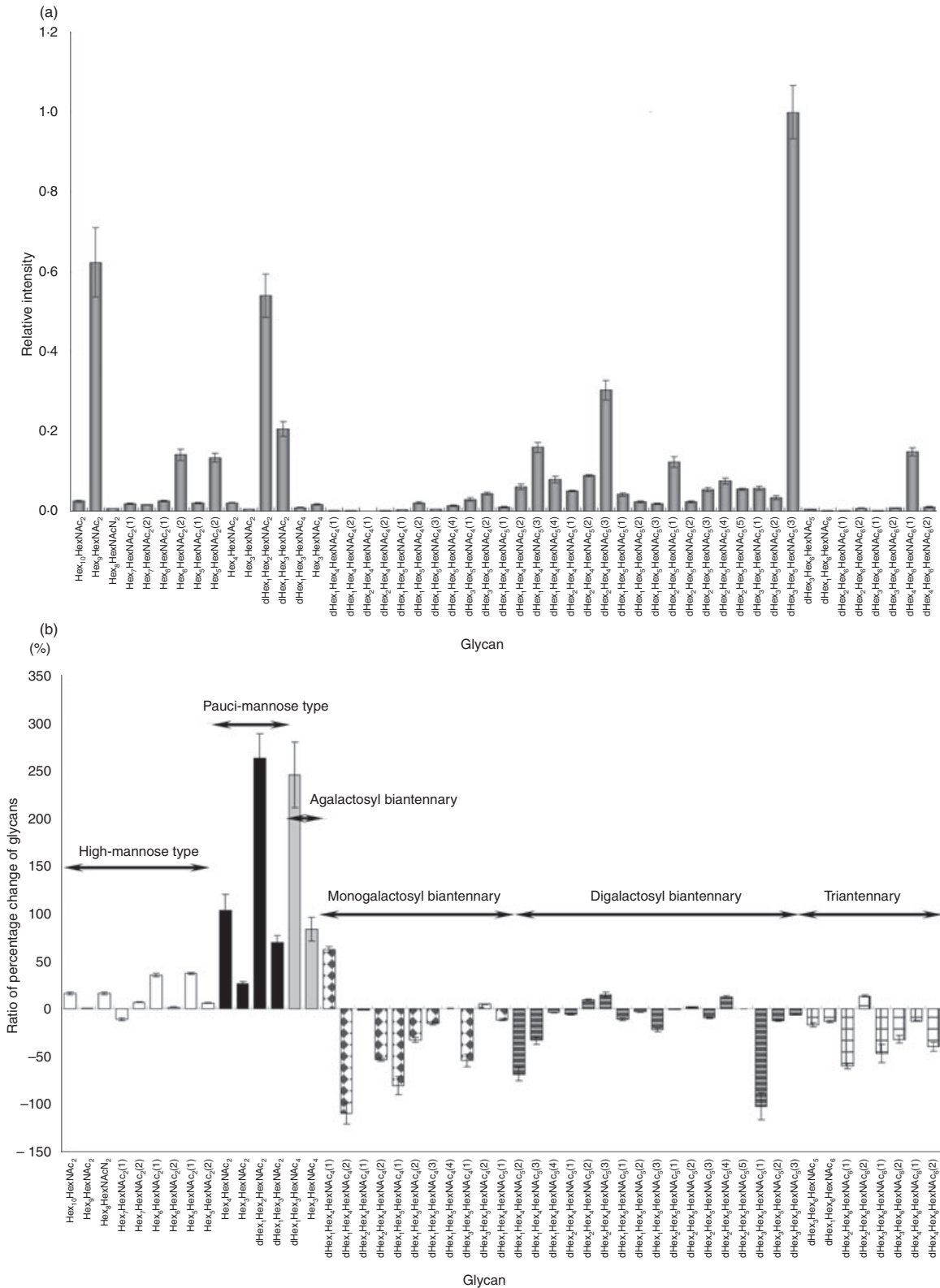
Figure 2. (a) Relative intensities of the molecular ions of d_0-pyridyl amino (PA) glycans from the systemic lupus erythematosus (SLE) model mouse. The intensity of the most intense ion ($[M + 2H]^{2+}$ of d_4-PA dHex$_3$Hex$_5$HexNAc$_3$(3), *m/z* 1180·97) was taken as 1·0. (b) Rate of percentage change of d_0/d_4-glycans. Each value is the average of three biological repeats. Error bars correspond to the standard deviation. The numbers in parentheses show the isomers.

molecular ions (Fig. 2b). The significant changes found in many glycans are described below.

Increased oligosaccharides in the SLE-model mouse

Figure 3(a,b) show the mass and MS/MS spectra of the most increased glycan, which showed a notable increase in the SLE-model mouse. Based on m/z values of molecular ions and differences of 1·00 U in m/z values among monoisotopic ions, the intense ion (m/z 973·40) and its neighbour ion (m/z 977·43) were assigned to $[M+H]^+$ of d_0-PA $dHex_1Hex_2HexNAc_2$, and d_4-PA $dHex_1Hex_2HexNAc_2$, respectively (Fig. 3a). The intensity ratio of these ions suggested that the level of $dHex_1Hex_2HexNAc_2$ increased 3·6-fold in the SLE-model mouse. The structure of this oligosaccharide was estimated to be a core-fucosylated trimannosyl core lacking a Man residue from the successive cleavages of Man (Y_3: m/z 815), Man (Y_2: m/z 653), GlcNAc (Y_1: m/z 450) and Fuc ($Y_{1/1'}$: m/z 304) (inset in Fig. 3b). Such a defective N-glycan is known as a paucimannose-type glycan, and is rarely found in vertebrates. All paucimannose-type glycans, such as $dHex_1$ $Hex_3HexNAc_2$ (a core-fucosylated trimannosyl core) and $Hex_3HexNAc_2$ (a non-fucosylated trimannosyl core) were increased in the SLE-model mouse. Furthermore, a two-fold increase was found in $Hex_4HexNAc_2$ (Man-4).

Figure 4 shows the molecular ratios of individual N-glycans between the SLE-model mice and control mice. A remarkable increase (3·5-fold) was also found in $dHex_1Hex_3HexNAc_4$, which is assigned to a core-fucosylated biantennary oligosaccharide lacking two non-reducing terminal Gal residues; its non-fucosylated form ($Hex_3HexNAc_4$) was also increased 1·8-fold in the SLE-model mouse. In other complex-type glycans, $dHex_1Hex_4HexNAc_4$ (1), which is assigned to a biantennary oligosaccharide lacking one molecule of Gal, increased 1·6-fold. Interestingly, a significant decrease was found in $dHex_1Hex_4HexNAc_4$ (2), a positional isomer of $dHex_1Hex_4HexNAc_4$ (1); this might have been caused by galactosylation on either GlcNAc-Manα1–3 or GlcNAc-Manα1–6. In contrast, no change was found between fucosylated and non-fucosylated oligosaccharides, nor between bisected and non-bisected oligosaccharides.

A significant increase was found in some high-mannose-type oligosaccharides, such as $Hex_5HexNAc_2$ (Man-5; + 137%) and $Hex_6HexNAc_2$ (1) (Man-6; + 136%), while $Hex_7HexNAc_2$ (1,2) (Man-7) and a positional isomer of $Hex_6HexNAc_2$ (1) [$Hex_6HexNAc_2$ (2)] remained unchanged in the SLE-model mouse. A slight increase was found in $Hex_8HexNAc_2$ (Man-8; + 116%) and $Hex_{10}HexNAc_2$ (possibly assigned to Man-9 plus Glc; + 116%).

Decreased oligosaccharides in the SLE-model mouse

The mass spectrum of the most decreased glycan is shown in Fig. 5(a). Based on differences of 0·5 U in m/z values among monoisotopic ions, molecular ions at m/z 1180·97
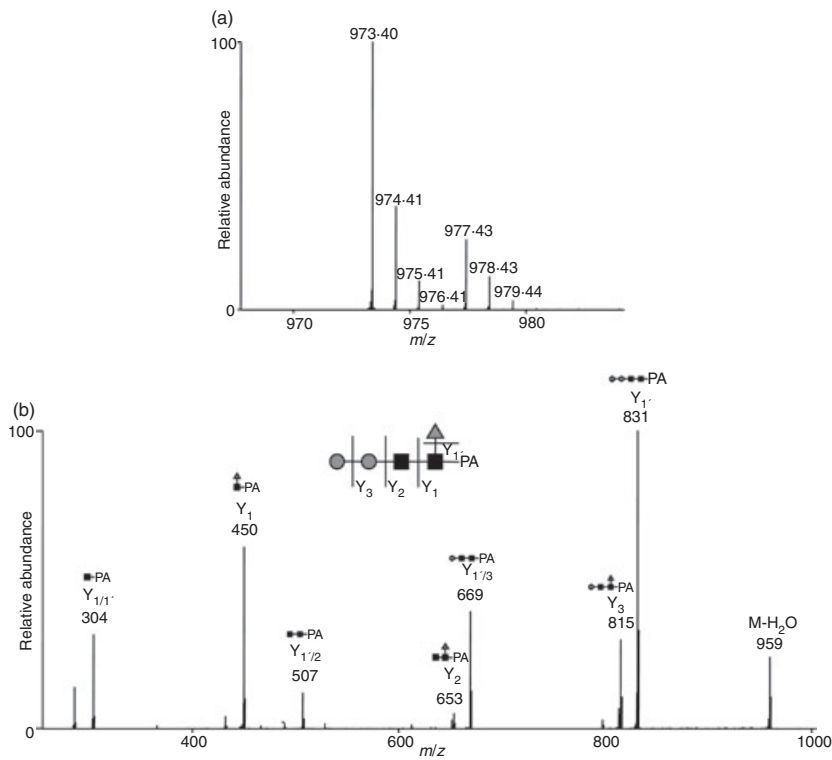

Figure 3. Mass (a) and mass spectrometry (MS)/MS (b) spectra of the most increased glycan ($dHex_1Hex_2HexNAc_2$). Precursor ion, m/z 973·4; grey circle, mannose; grey triangle, fucose; black square, N-acetylglucosamine.

Increased glycan (>120%)	Deduced structure								
Abbreviation	$Hex_6HexNAc_2$ (1)	$Hex_5HexNAc_2$ (1)	$Hex_4HexNAc_2$	$Hex_3HexNAc_2$	$dHex_1Hex_2HexNAc_2$	$dHex_1Hex_3HexNAc_2$	$Hex_3HexNAc_4$	$dHex_1Hex_3HexNAc_4$	$dHex_1Hex_4HexNAc_4$ (1)
Intensity ratio(%)	136	137	204	139	363	170	184	346	163

Decreased glycan (<−120%)	Deduced structure								
Abbreviation	$dHex_1Hex_4HexNAc_4$ (2)	$dHex_1Hex_4HexNAc_5$ (1,2)	$dHex_1Hex_5HexNAc_4$ (1,2)	$dHex_2Hex_4HexNAc_4$ (2)	$dHex_2Hex_4HexNAc_5$ (1)	$dHex_3Hex_5HexNAc_5$ (1)	$dHex_2Hex_5HexNAc_6$ (1)	$dHex_3Hex_6HexNAc_6$ (1,2)	$dHex_4Hex_6HexNAc_6$ (2)
Intensity ratio(%)	−208	−182, −133	−169, −133	−149	−154	−213	−159	−147, −132	−139

Other glycan	Deduced structure								
Abbreviation	$Hex_{10}HexNAc_2$	$Hex_9HexNAc_2$	$Hex_8HexNAc_2$	$Hex_7HexNAc_2$ (1,2)	$Hex_6HexNAc_2$ (2)	$Hex_5HexNAc_2$ (2)	$dHex_1Hex_4HexNAc_5$ (3,4)	$dHex_2Hex_4HexNAc_4$ (1)	$dHex_2Hex_4HexNAc_5$ (2,3)
Intensity ratio (%)	116	101	116	−111, 107	102	106	−115, 101	−101	105, −111
Deduced structure									
Abbreviation	$dHex_1Hex_5HexNAc_4$ (3,4)	$dHex_1Hex_5HexNAc_5$ (1–3)	$dHex_2Hex_5HexNAc_5$ (1–5)	$dHex_3Hex_5HexNAc_4$ (1,2)	$dHex_3Hex_5HexNAc_5$ (2,3)	$dHex_3Hex_6HexNAc_5$	$dHex_1Hex_6HexNAc_6$	$dHex_2Hex_6HexNAc_6$ (2)	$dHex_4Hex_6HexNAc_6$ (1)
Intensity ratio(%)	−104, −105	−111, −103, −119	−101, 102, −110, 113, 100	110, 115	−112	−106	−114	116	−112

Figure 4. Summary of quantitative analysis of the systemic lupus erythematosus (SLE) model mouse against control mice. Values of relative ratios are the averages of three biological repeats. Grey circle, mannose; white circle, galactose; grey triangle, fucose; black square, *N*-acetylglucosamine.

and 1182·98 are estimated to be $[M + 2H]^{2+}$ of d_0-PA and d_4-PA $dHex_3Hex_5HexNAc_5$ (1), respectively. The intensity ratio of $d_0 : d_4$ glycans suggests that this glycan in the SLE-model mouse was decreased to 47% of the amount found in the control mouse. Figure 5(b) shows the $MS^{2–4}$ spectra of d_0-PA $dHex_3Hex_5HexNAc_5$ (1) (precursor ion, *m/z* 1180·97). The fragment ion at *m/z* 512 in MS/MS (i) and MS/MS/MS (ii) spectra, which corresponds to $dHex_1Hex_1HexNAc_1^+$, suggests the attachment of two Lewis motifs on the side chains of the glycan. The presence of $dHex_1HexNAc_1PA^+$ (*m/z* 446) and $dHex_1Hex_1HexNAc_3PA^+$ (*m/z* 1015) reveals the linkages of a core fucose and a bisecting GlcNAc. Based on these fragments, this decreased glycan is estimated to be a Lewis-motif-modified, core-fucosylated and bisected biantennary oligosaccharide (inset in Fig. 5).

As shown in Figs 2(b) and 4, oligosaccharides lacking one molecule of Gal with and without bisecting Glc-NAc [$dHex_1Hex_4HexNAc_4$ (2) and $dHex_1Hex_4HexNAc_5$ (1)] were decreased to 48% and 55%, respectively. A significant decrease was also found in other monogalacto-biantennary oligosaccharides, such as $dHex_2Hex_4Hex$ NAc_4 (2) (a Lewis-motif-modified, core-fucosylated monogalacto-biantennary) and $dHex_2Hex_4HexNAc_5$ (1) (a Lewis-motif-modified core-fucosylated and bisected monogalacto-biantennary).

The oligosaccharides, non-reducing ends of which are fully galactosylated, were decreased in the SLE-model mouse. For example, monofucosyl biantennary $dHex_1Hex_5HexNAc_4$ (1) and (2) were decreased 59% and 75%, respectively. The di-, tri- and tetra-fucosylated oligosaccharides, $dHex_2Hex_6HexNAc_6$ (1), $dHex_3Hex_6Hex$-NAc_6 (1,2) and $dHex_4Hex_6HexNAc_6$ (1,2), which were estimated to be tri- and tetraantennary forms, were also significantly decreased. These results show that oligosaccharides with a complicated structure, such as high branching oligosaccharides and di- and tri-fucosylated oligosaccharides, were decreased in the SLE-model mouse.

Discussion

Using the isotope-tagging method, we demonstrated aberrant *N*-glycosylation on the kidney proteins of a SLE-model mouse. We found increases in low-molecular-mass glycans with simple structures, including paucimannose-type glycans, agalacto-biantennary oligosaccharides, Man-5 and Man-6, and decreases in glycans which have a complicated and diverse structure, such as digalacto-biantennary oligosaccharides and highly fucosylated glycans (Fig. 4). An increase in agalacto-biantennary oligosaccharides on IgG has been reported in the sera of patients with autoimmune diseases, including SLE, rheumatoid arthritis and IgA
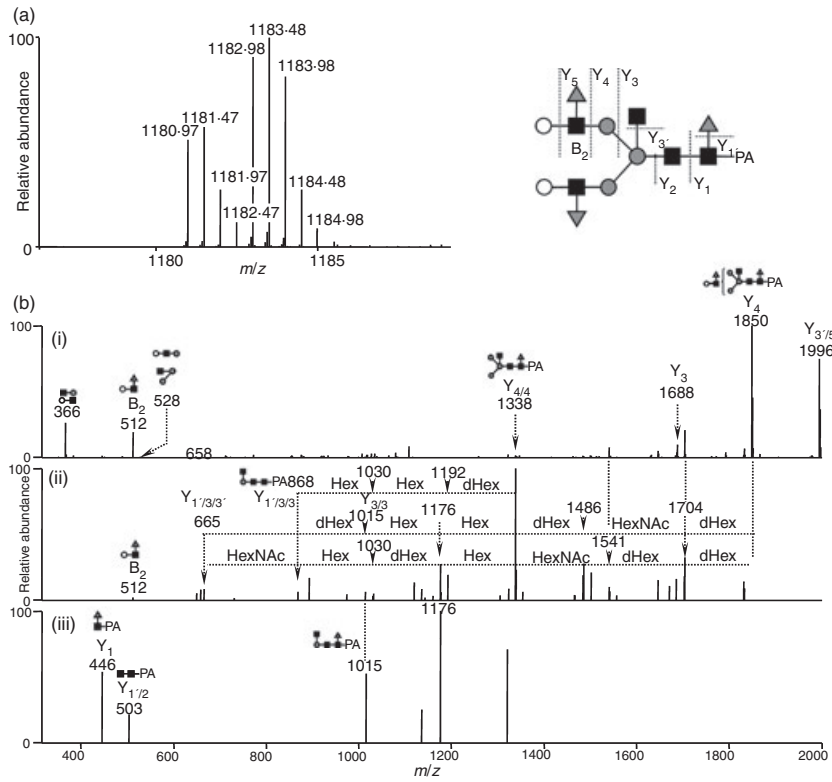
Figure 5. (a) Mass spectrum of the most decreased glycan [dHex$_3$Hex$_5$HexNAc$_5$ (1)]; (b-i) Mass spectrometry (MS)/MS spectrum of *m/z* 1181·0; (b-ii) MS/MS/MS spectrum of *m/z* 1849·7; (b-iii) MS/MS/MS/MS spectrum of *m/z* 1338·3. Grey circle, mannose; white circle, galactose; grey triangle, fucose; black square, *N*-acetylglucosamine; dHex, deoxyhexose (fucose); Hex, hexose (mannose and galactose); HN, *N*-acetylhexosamine (*N*-acetylglucosamine).

nephropathy.[9,11,28] The present findings show that abnormal glycosylation occurs not only in IgG in serum but also in several glycoproteins in the SLE-model mouse kidney.

Figure 6 shows the biosynthesis pathway of *N*-linked oligosaccharides in mammalian cells. Man-9, a product in the early stage of the pathway, is processed to Man-5 in the endoplasmic reticulum, and a GlcNAc and Fuc are added to Man-5 in the Golgi apparatus. After the removal of two Man residues by αM-II, GlcNAc, Gal and Fuc are further added to oligosaccharides by several glycosyltransferases. There have been a few reports on paucimannose-type oligosaccharides in vertebrates;[29] however, these glycans are common oligosaccharides in other multicellular organisms such as insects and *Caenorhabditis*

elegans.[30,31] The membrane protease β-*N*-acetylglucosaminidase is thought to mediate the synthesis of paucimannose-type oligosaccharides.[32] Based on core fucosylation on some paucimannose-type oligosaccharides, it was deduced that β-*N*-acetylglucosaminidase might act on glycan synthesis after *N*-acetylglucosaminyltransferase I, core fucosyltransferase and αM-II.[32] The synthesis of paucimannose-type oligosaccharides may be involved in the suppression of growing diversity and complexity of glycan structures.

We found a number of changes in the levels of monogalacto-biantennary oligosaccharides in the SLE mouse. Galactosylation to agalacto-biantennary oligosaccharides is mediated by β-1,4-galactosyltransferase
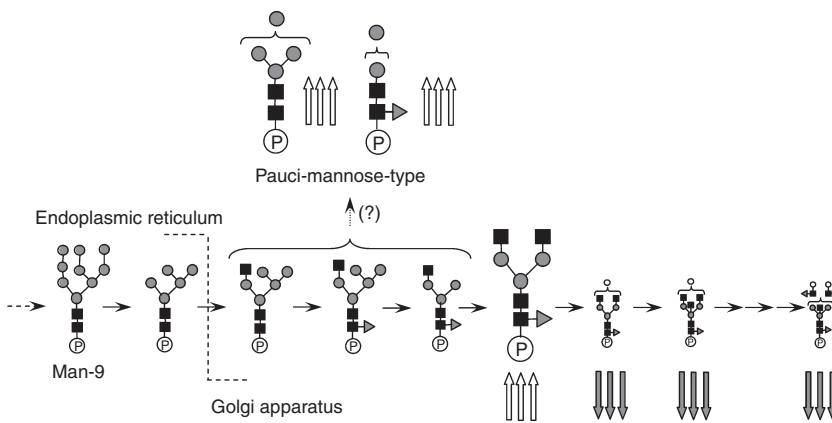

Figure 6. Biosynthesis pathway of *N*-linked oligosaccharides in mammalian cells. Triple up-arrow, increases of more than +2·0; triple down-arrow, decreases of not more than −2·0. Grey circle, mannose; white circle, galactose; grey triangle, fucose; black square, *N*-acetylglucosamine. 'P' is protein portion.

(β-1,4-GalTase).[33] Previous studies suggested that translational repression of β-1,4-GalTase in lymphocytes is associated with an increase in agalacto-oligosaccharides on IgG in the serum of the MRL-lpr mouse.[34] Although the activity of β-1,4-GalTase remains unknown in the SLE-model mouse, the increase in agalacto forms and the decrease in digalacto forms imply changes in β-1,4-GalTase activity. The present results suggest a decrease in diverse and complex glycans, which are synthesized at a late stage in the *N*-glycan synthesis pathway, and an increase in the simple glycans appearing at an early stage in the SLE-model mouse.

The activation of complements is involved in glomerular nephritis of SLE.[35–37] The complements are activated through three pathways: a classical pathway, an alternative pathway and a lectin pathway. In the classical pathway, a binding of C1q to an immune complex triggers the activation of C1r and C1s. Activated C1s cleaves C4 and C2, generating C3 convertase (C4b2a), which generates C3b. The complement component subsequently produces C5b-9 complex, which leads to an inflammatory response on host tissues.[38–41] The excess deposition of immune complexes followed by a sustained immune response triggers tissue disorders, including lupus nephritis.[42–45] In the lectin pathway, mannose-binding lectin (MBL) is associated with the activation of complements. Two forms of MBL (MBL-A and MBL-C) are present in complexes with MBL-associated serine proteases (MASPs) in mice. The MASPs are activated by binding MBL to Man or GlcNAc on the surface of the antigen in a calcium-dependent manner.[46–49] Like C1s in the classical pathway, activated MASPs cleave C4 and C2.[50,51] In lupus nephritis, MBL-A and MBL-C in the immune complex bind to GlcNAc residues at the reducing ends of agalacto-biantennary oligosaccharides in IgG,[52] and subsequently activate the complements.[53,54] In αM-II-deficient mice, which suffer from SLE-like syndromes including kidney disorders, the majority of glycans are hybrid-type oligosaccharides because of the failure of Man trimming by the lack of αM-II.[16] Green *et al.* concluded that MBL recognized Manα1–3 and Manα1–6 linkages in hybrid-type oligosaccharides,[17] and glycans lacking normal side chains, including agalacto-biantennary oligosaccharides, might be involved in the aberrant immune response in autoimmune diseases. Paucimannose glycans, which contain exposed Manα1–3 or Manα1–6 linkages, may be recognized as ligand carbohydrates by MBL. Our present finding, an increase in paucimannose oligosaccharides and agalacto forms, might result from an alteration of the biosynthesis pathway of *N*-glycans. The alterations may cause the aberrant glycosylations on most of the glycoproteins rather than some glycoproteins in the SLE-model mouse. The changes in glycosylation might be involved in an autoimmune pathogenesis in the SLE-model mouse kidney.

The continuous production of aberrant antibodies that react with components from self-tissue and accumulation in the immune complex are thought to promote tissue damage in autoimmune disease.[55,56] The mechanism of localized accumulation in the immune complex in some tissues remains unknown in SLE. We found an increase in glycans that may bind to MBL and subsequently promote complement activation via the lectin pathway in the mouse kidney. Our present results suggest that an aberrant *N*-glycan synthesis pathway as well as an abnormal immune system may be involved in the damage caused by glomerular nephritis in the SLE-model mouse.

Acknowledgements

References

1 Dwek RA. Glycobiology: toward understanding the function of sugars. *Chem Rev* 1996; **96**:683–720.

2 Helenius A, Aebi M. Intracellular functions of N-linked glycans. *Science* 2001; **291**:2364–9.

3 Zak I, Lewandowska E, Gnyp W. Selectin glycoprotein ligands. *Acta Biochim Pol* 2000; **47**:393–412.

4 Axford JS. Glycosylation and rheumatic disease. *Biochim Biophys Acta* 1999; **1455**:219–29.

5 Feizi T, Gooi HC, Childs RA, Picard JK, Uemura K, Loomes LM, Thorpe SJ, Hounsell EF. Tumour-associated and differentiation antigens on the carbohydrate moieties of mucin-type glycoproteins. *Biochem Soc Trans* 1984; **12**:591–6.

6 Kannagi R, Izawa M, Koike T, Miyazaki K, Kimura N. Carbohydrate-mediated cell adhesion in cancer metastasis and angiogenesis. *Cancer Sci* 2004; **95**:377–84.

7 Goodarzi MT, Turner GA. Decreased branching, increased fucosylation and changed sialylation of alpha-1-proteinase inhibitor in breast and ovarian cancer. *Clin Chim Acta* 1995; **236**:161–71.

8 Yamashita K, Fukushima K, Sakiyama T, Murata F, Kuroki M, Matsuoka Y. Expression of Sia alpha 2→6Gal beta 1→4GlcNAc residues on sugar chains of glycoproteins including carcinoembryonic antigens in human colon adenocarcinoma: applications of *Trichosanthes japonica* agglutinin I for early diagnosis. *Cancer Res* 1995; **55**:1675–9.

9 Tomana M, Schrohenloher RE, Reveille JD, Arnett FC, Koopman WJ. Abnormal galactosylation of serum IgG in patients with systemic lupus erythematosus and members of families with high frequency of autoimmune diseases. *Rheumatol Int* 1992; **12**:191–4.

10 Mizuochi T, Hamako J, Nose M, Titani K. Structural changes in the oligosaccharide chains of IgG in autoimmune MRL/Mp-lpr/lpr mice. *J Immunol* 1990; **145**:1794–8.

11 Arnold JN, Wormald MR, Sim RB, Rudd PM, Dwek RA. The impact of glycosylation on the biological function and structure

of human immunoglobulins. *Annu Rev Immunol* 2007; **25**:21–50.

12 Das H, Atsumi T, Fukushima Y *et al.* Diagnostic value of anti-agalactosyl IgG antibodies in rheumatoid arthritis. *Clin Rheumatol* 2004; **23**:218–22.

13 Raghav SK, Gupta B, Agrawal C, Saroha A, Das RH, Chaturvedi VP, Das HR. Altered expression and glycosylation of plasma proteins in rheumatoid arthritis. *Glycoconj J* 2006; **23**:167–73.

14 Elliott MA, Elliott HG, Gallagher K, McGuire J, Field M, Smith KD. Investigation into the concanavalin A reactivity, fucosylation and oligosaccharide microheterogeneity of alpha 1-acid glycoprotein expressed in the sera of patients with rheumatoid arthritis. *J Chromatogr B Biomed Sci Appl* 1997; **688**:229–37.

15 Rops AL, van den Hoven MJ, Bakker MA *et al.* Expression of glomerular heparan sulphate domains in murine and human lupus nephritis. *Nephrol Dial Transplant* 2007; **22**:1891–902.

16 Chui D, Sellakumar G, Green R *et al.* Genetic remodeling of protein glycosylation *in vivo* induces autoimmune disease. *Proc Natl Acad Sci USA* 2001; **98**:1142–7.

17 Green RS, Stone EL, Tenno M, Lehtonen E, Farquhar MG, Marth JD. Mammalian *N*-glycan branching protects against innate immune self-recognition and inflammation in autoimmune disease pathogenesis. *Immunity* 2007; **27**:308–20.

18 Wada Y. Mass spectrometry in the detection and diagnosis of congenital disorders of glycosylation. *Eur J Mass Spectrom (Chichester, Eng)* 2007; **13**:101–3.

19 Faid V, Chirat F, Seta N, Foulquier F, Morelle W. A rapid mass spectrometric strategy for the characterization of *N*- and *O*-glycan chains in the diagnosis of defects in glycan biosynthesis. *Proteomics* 2007; **7**:1800–13.

20 Miyamoto S. Clinical applications of glycomic approaches for the detection of cancer and other diseases. *Curr Opin Mol Ther* 2006; **8**:507–13.

21 Yuan J, Hashii N, Kawasaki N, Itoh S, Kawanishi T, Hayakawa T. Isotope tag method for quantitative analysis of carbohydrates by liquid chromatography-mass spectrometry. *J Chromatogr A* 2005; **1067**:145–52.

22 Alvarez-Manilla G, Warren NL, Abney T, Atwood J III, Azadi P, York WS, Pierce M, Orlando R. Tools for glycomics: relative quantitation of glycans by isotopic permethylation using 13CH3I. *Glycobiology* 2007; **17**:677–87.

23 Kang P, Mechref Y, Kyselova Z, Goetz JA, Novotny MV. Comparative glycomic mapping through quantitative permethylation and stable-isotope labeling. *Anal Chem* 2007; **79**:6064–73.

24 Bowman MJ, Zaia J. Tags for the stable isotopic labeling of carbohydrates and quantitative analysis by mass spectrometry. *Anal Chem* 2007; **79**:5777–84.

25 Watanabe-Fukunaga R, Brannan CI, Copeland NG, Jenkins NA, Nagata S. Lymphoproliferation disorder in mice explained by defects in Fas antigen that mediates apoptosis. *Nature* 1992; **356**:314–7.

26 Adachi M, Watanabe-Fukunaga R, Nagata S. Aberrant transcription caused by the insertion of an early transposable element in an intron of the Fas antigen gene of lpr mice. *Proc Natl Acad Sci USA* 1993; **90**:1756–60.

27 Merino R, Iwamoto M, Fossati L, Izui S. Polyclonal B cell activation arises from different mechanisms in lupus-prone (NZB × NZW)F$_1$ and MRL/MpJ-lpr/lpr mice. *J Immunol* 1993; **151**:6509–16.

28 Homma H, Tozawa K, Yasui T, Itoh Y, Hayashi Y, Kohri K. Abnormal glycosylation of serum IgG in patients with IgA nephropathy. *Clin Exp Nephrol* 2006; **10**:180–5.

29 Hase S, Okawa K, Ikenaka T. Identification of the trimannosyl-chitobiose structure in sugar moieties of Japanese quail ovomucoid. *J Biochem* 1982; **91**:735–7.

30 Kubelka V, Altmann F, Kornfeld G, Marz L. Structures of the N-linked oligosaccharides of the membrane glycoproteins from three lepidopteran cell lines (Sf-21, IZD-Mb-0503, Bm-N). *Arch Biochem Biophys* 1994; **308**:148–57.

31 Natsuka S, Adachi J, Kawaguchi M, Nakakita S, Hase S, Ichikawa A, Ikura K. Structural analysis of N-linked glycans in *Caenorhabditis elegans*. *J Biochem* 2002; **131**:807–13.

32 Altmann F, Schwihla H, Staudacher E, Glossl J, Marz L. Insect cells contain an unusual, membrane-bound beta-*N*-acetylglucosaminidase probably involved in the processing of protein *N*-glycans. *J Biol Chem* 1995; **270**:17344–9.

33 Guo S, Sato T, Shirane K, Furukawa K. Galactosylation of N-linked oligosaccharides by human beta-1,4-galactosyltransferases I, II, III, IV, V, and VI expressed in Sf-9 cells. *Glycobiology* 2001; **11**:813–20.

34 Jeddi PA, Lund T, Bodman KB *et al.* Reduced galactosyltransferase mRNA levels are associated with the agalactosyl IgG found in arthritis-prone MRL-lpr/lpr strain mice. *Immunology* 1994; **83**:484–8.

35 Cameron JS. Lupus nephritis. *J Am Soc Nephrol* 1999; **10**:413–24.

36 Walport MJ. Complement. First of two parts. *N Engl J Med* 2001; **344**:1058–66.

37 Walport MJ. Complement. Second of two parts. *N Engl J Med* 2001; **344**:1140–4.

38 Botto M. Links between complement deficiency and apoptosis. *Arthritis Res* 2001; **3**:207–10.

39 Hanayama R, Tanaka M, Miyasaka K, Aozasa K, Koike M, Uchiyama Y, Nagata S. Autoimmune disease and impaired uptake of apoptotic cells in MFG-E8-deficient mice. *Science* 2004; **304**:1147–50.

40 Arason GJ, Steinsson K, Kolka R, Vikingsdottir T, D'Ambrogio MS, Valdimarsson H. Patients with systemic lupus erythematosus are deficient in complement-dependent prevention of immune precipitation. *Rheumatology (Oxford)* 2004; **43**:783–9.

41 Cook HT, Botto M. Mechanisms of disease: the complement system and the pathogenesis of systemic lupus erythematosus. *Nat Clin Pract Rheumatol* 2006; **2**:330–7.

42 Gunnarsson I, Sundelin B, Heimburger M, Forslid J, van Vollenhoven R, Lundberg I, Jacobson SH. Repeated renal biopsy in proliferative lupus nephritis – predictive role of serum C1q and albuminuria. *J Rheumatol* 2002; **29**:693–9.

43 Buyon JP, Tamerius J, Belmont HM, Abramson SB. Assessment of disease activity and impending flare in patients with systemic lupus erythematosus. Comparison of the use of complement split products and conventional measurements of complement. *Arthritis Rheum* 1992; **35**:1028–37.

44 Markiewski MM, Lambris JD. The role of complement in inflammatory diseases from behind the scenes into the spotlight. *Am J Pathol* 2007; **171**:715–27.

45 Sturfelt G. The complement system in systemic lupus erythematosus. *Scand J Rheumatol* 2002; **31**:129–32.

46 Holmskov U, Malhotra R, Sim RB, Jensenius JC. Collectins: collagenous C-type lectins of the innate immune defense system. *Immunol Today* 1994; **15**:67–74.

47 Weis WI, Drickamer K, Hendrickson WA. Structure of a C-type mannose-binding protein complexed with an oligosaccharide. *Nature* 1992; **360**:127–34.

48 Takahashi M, Mori S, Shigeta S, Fujita T. Role of MBL-associated serine protease (MASP) on activation of the lectin complement pathway. *Adv Exp Med Biol* 2007; **598**:93–104.

49 Turner MW. Mannose-binding lectin: the pluripotent molecule of the innate immune system. *Immunol Today* 1996; **17**:532–40.

50 Holmskov U, Malhotra R, Sim RB, Jensenius JC. Collectins: collagenous C-type lectins of the innate immune defense system. *Immunol Today* 1994; **15**:67–74.

51 Thiel S, Vorup-Jensen T, Stover CM *et al.* A second serine protease associated with mannan-binding lectin that activates complement. *Nature* 1997; **386**:506–10.

52 Lhotta K, Wurzner R, Konig P. Glomerular deposition of mannose-binding lectin in human glomerulonephritis. *Nephrol Dial Transplant* 1999; **14**:881–6.

53 Ohsawa I, Ohi H, Tamano M *et al.* Cryoprecipitate of patients with cryoglobulinemic glomerulonephritis contains molecules of the lectin complement pathway. *Clin Immunol* 2001; **101**:59–66.

54 Trouw LA, Seelen MA, Duijs JM *et al.* Activation of the lectin pathway in murine lupus nephritis. *Mol Immunol* 2005; **42**:731–40.

55 Jorgensen TN, Gubbels MR, Kotzin BL. New insights into disease pathogenesis from mouse lupus genetics. *Curr Opin Immunol* 2004; **16**:787–93.

56 Lauwerys BR, Wakeland EK. Genetics of lupus nephritis. *Lupus* 2005; **14**:2–12.